Research Article • DOI: 10.2478/amst-2019-0018 AMST • 44(4) • 2020 • 113–120

sciendo

Advances in Manufacturing Science and Technology

Decarbonizing of Ductile Cast Iron Surface for Usage in Two-Layered Casting

Grzegorz Rzepka, Jacek Nawrocki*, Jan Sieniawski

Department of Materials Science, Faculty of Mechanical Engineering and Aeronautics, Rzeszow University of Technology, Powstańców Warszawy 12, 35-959 Rzeszów, Poland

Abstract

The main purpose of the present study is to verify the possibility of decarbonizing the surface of heat-resistant ductile iron GJS-XSiMo5-1 to provide a significant difference in carbon content between this material and gray cast iron EN-GJL-250. In the future, this will allow to increase the diffusion of elements during the creation of the two-layered material using the casting process with materials in a liquid state and solid state. The above method was assumed to solve the problem of defects on turbocharger's housing in an economically justified manner which occurred in some high-performance premium applications. Evaluation of decarbonized surface quality was investigated by microstructure observation (light microscopy) and alloy elements diffusion (scanning electron microscopy), and hardness measurement and the element content were checked by spark optical emission spectrometry and glow discharge optical emission spectrometry, respectively.

Keywords

decarbonizing, heat-resistant ductile iron, two-layered material, casting

1. Introduction

Designers of internal combustion engines and propulsion systems are currently facing new challenges of the EU directive limiting the emission of harmful substances, primarily CO_2. Each car manufacturer proposes engines with higher performance. Analysis of literature data [1,2] indicates that the achievement of the requirements set for constructors and car manufacturers by the Euro 6D standard can be obtained by increasing ecological and economic effects resulting from the use of a turbocharger as a device supporting the operation of an internal combustion engine (Figure 1). It is a rotor-flow machine driven by the exhaust gases of the engine and its function is to increase the mass of air supplied per unit of time to the engine cylinders. Thus, it enables more accurate combustion of a larger mass of fuel, thus obtaining greater power and efficiency of the engine while limiting the emission of harmful chemical compounds in exhaust gases.

Currently, to increase the efficiency and power of internal combustion, engines for premium passenger cars often use an increase in exhaust gas temperature (up to a temperature of 1,050°C for gasoline-powered engines) flowing from moving engine cylinders and driving a turbocharger turbine. Increasing the heat energy supplied with the exhaust gases simultaneously leads to an increase in temperature and thermo-mechanical stresses occurring in individual turbocharger components and subassemblies.

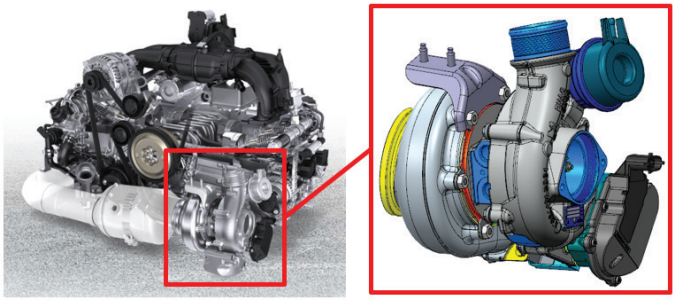

Figure 1. Internal combustion engine with a turbocharger.

Gray cast iron EN-GJL-250 is widely used as the material of bearing housing of turbocharger. It has some important benefits such as good castability, machinability, and corrosion resistance. It is also characterized by high damping capacity, low melting point, relatively low cost [3], and a relatively small resistance to thermal stresses (190 MPa in 500°C). It was found that the thermo-mechanical stresses occurring in the turbocharger housing are higher than the tensile strength of the widely used gray iron EN-GJL-250 used for a certain group of premium class

* *Corresponding author: Jacek Nawrocki*
E-mail: jaceknaw@prz.edu.pl

projects during a long-term thermo-mechanical fatigue (TMF) test. Hence, the impact of these stresses leads to cracking of the turbocharger bearing housing flange and causes leakage of the turbine system during increased operating conditions (Figure 2).

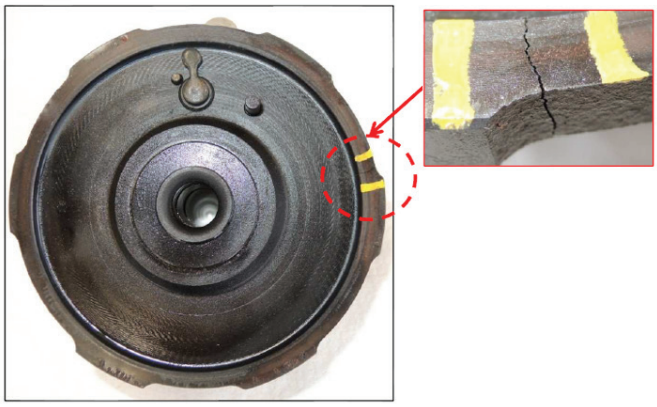

Figure 2. Breakage of the flange of bearing housing.

It can be assumed that the simplest solution to prevent casting from breakages in the case described earlier could be using the higher grade material such as heat-resistant ductile iron. The mentioned solution is not optimal from an economical point of view. The analysis of the results of previous experimental research conducted internally by turbocharger manufacturing company BorgWarner indicates that the increase in heat fatigue resistance of turbocharger components exposed to high-temperature exhaust gas is possible only by introducing the bearing housing flange material with a higher tensile strength at elevated temperature. The assumption can be realized by providing a two-layered material, consisting of the gray cast iron EN-GJL-250 in the bearing housing area and new, more heat-resistant material in the housing flange area where the heat flux from turbine stage of turbocharger is increased.

The two-layered material can be manufactured using several methods. The commonly used method is the welding process [4]. Although the process is well-known, it is quite expensive in mass production, the smooth surface of joint is required, and cracks are common at the weld interface. Another method which is similar to welding, also regarding restrictions, is vacuum brazing [5]. Additionally, it requires precisely machined surfaces for the joint. The so-called hot diffusion–compression bonding method can also be used to produce the two-layered materials [6]. In this process, two materials in the solid state are compressed in high temperatures to allow the creation of the bond. This method is restricted to small components with simple shapes. The preparation of the surface for the joint is necessary. The next wide group of methods to produce two-layered material is casting. There are two main types of this process. The first type is using two liquid alloys (liquid–liquid) that are poured into casting mold one after the other [7–9] or simultaneously in vertical direction without mixing of input materials [10]. The benefit of this method is that there is no need to prepare the surface for joint, but if the mold is complicated there is a need to control the processing temperature (by using thermocouples) and the surface of the joint has to be plain (gravitationally required). The second type of casting method uses one of the materials in the solid state, placing it in the form and pouring on it the second material in a liquid state (solid–liquid) [11–16]. This process allows to provide the complex surface of the joint (as the shape of the material in solid state). Modification of the earlier described process is using the material in the powder state which is placed in the mold and then poured with liquid material [4, 17, 18].

From the economical point of view, the best solution to resolve the problem discussed is solid–liquid casting process. To substantially increase of heat resistance, ductile iron GJS-XSiMo5-1 has been selected. The review of the literature indicates that limited information considering joining of materials EN-GJL-250/GJS-XSiMo5-1 is available. The focus of scientific literature is on joining gray cast iron with different types of cast iron dedicated to work in low/ambient temperature [7, 9, 11, 19–23]. The literature data suggest that good quality joining of materials from group Fe–C is determined if the significant difference of carbon content (ΔC) between joined materials occurs. Depending on the different casting parameters, the value of difference varies from 1.0 to 2.0 wt.% [23]. This requirement for materials GJL-250/GJS-XSiMo5-1 (ΔC: from 0.0 to 0.7 wt.%) is not fulfilled.

The main objective of the present study is to verify the possibility of decarbonizing the surface of heat-resistant ductile iron GJS-XSiMo5-1 to provide a significant difference in carbon content between this material and gray cast iron EN-GJL-250. In the future, this will allow to increase the diffusion of elements during the creation of the two-layered material using the casting process with materials in a liquid state and solid state. The evaluation of decarbonized surface quality was investigated by microstructure observation using light microscope (LM), and hardness measurement and the element content were checked by spark optical emission spectrometry (spark-OES) and glow discharge optical emission spectrometry (GD-OES), respectively.

2. Material and Experiment

The tests of decarbonizing process on the surface of ductile iron GJS-XSiMo5-1 (chemical composition (wt.%): C, 3.3; Mn, 0.6; Si, 4.3; Mo, 0.9; P, 0.1; S, 0.01; Mg, 0.5; Fe, balanced) were prepared according to the plan proposed in Figure 3.

Decarbonizing tests were performed on the test stand containing resistance furnace, gas-blowing device, and temperature recorder with sheathed control thermocouple S-type with diameter 1.5 mm (Figure 4).

Trials with diameter 50 mm and height 15 mm were drilled in the trial axis with bores (diameter 2 mm and depth 3 mm). The specimen surface was ultrasonically washed in isopropyl alcohol (10 min) and dried. The specimen was put in the resistance furnace, and a thermocouple was installed in the drilled hole. After turning on the gas-blowing device, the furnace was activated and the decarbonizing process was provided according to Table 1.

Cross-section of the material was prepared using standard metallographic mechanical grinding and polishing techniques. LM observations were performed using a Leica DM3000 microscope with an automatic image analysis program LAS V4.9. Scanning electron microscopic (SEM) observations were conducted using a Hitachi S-3400N microscope. Hardness was measured by the Brinell method using Zwick ZHU 250 device (ball diameter 2.5 mm and pressure force 187.5 N). Additionally, the spark-OES ARL 3460 was used to analyze the element content and the GD-OES GDS GD PROFILER HR was used to check the difference of element content as a function of depth (distance from surface).

3. Results and Discussion

The analysis of changes in the carbon content in the surface layer was carried out using the Student's *t*-test at the confidence level 1 – " = 95% for comparison. The results are shown in Figure 5. The change in carbon content was determined as statistically significant for all decarburization processes. The assumed acceptance criterion was met—obtaining a carbon content in the surface layer below 1.9 wt.%—for decarburization process no. 2 (T = 1,123 K, Ar 100%, τ = 2 h) 1.8 wt.% and for process no. 6 (T = 1,123 K, Ar 100%, τ = 6 h) 1.7 wt.%. Additional goal—achieving a 1.7 wt.% change in carbon content after the decarburization process in relation to the value before the process—was met for all the presented process conditions, except for process no. 5 (T = 973 K, Ar 20% + CO_2 80%, τ = 6 h). The largest change in carbon content was observed for process no. 6 (T = 1,123 K, Ar 100%, τ = 6 h)—3.4 wt.% and the smallest for process no. 5 (T = 973 K, Ar 20% + CO_2 80%, τ = 6 h)—1.1 wt.%.

The depth of the decarbonized layer and decarbonizing factor were defined in accordance with the profile of change of carbon content in the function of depth (distance from the surface; Table 2 and Figures 6–10). The decarbonizing factor was measured as the surface area of the region above the curve corresponding to the decarbonizing process and it was shown as a dimensionless value. Corrosion products on the

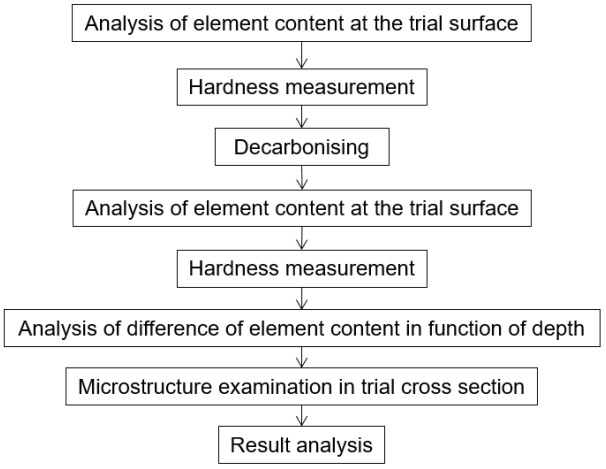

Figure 3. Test plan of decarbonizing process.

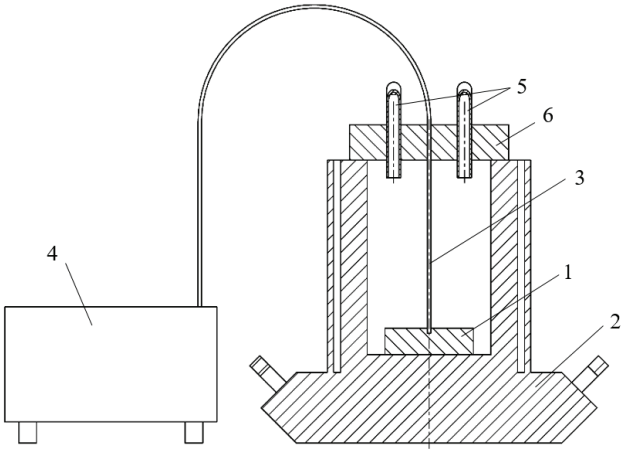

Figure 4. Decarbonizing test stand. (1) Specimen, (2) furnace, (3) thermocouple, (4) recorder, (5) gas-blowing device, and (6) cover.

Table 1. Parameters of decarbonizing process

Process no.	Decarbonizing process		
	Temperature (K)	Gas mixture composition	Time (h)
1	Reference specimen—as cast state		
2	1,123	Ar 100%	2
3	1,123	Ar 70% + CO_2 30%	2
4	973	Ar 20% + CO_2 80%	2
5	973	Ar 20% + CO_2 80%	6
6	1,123	Ar 100%	6

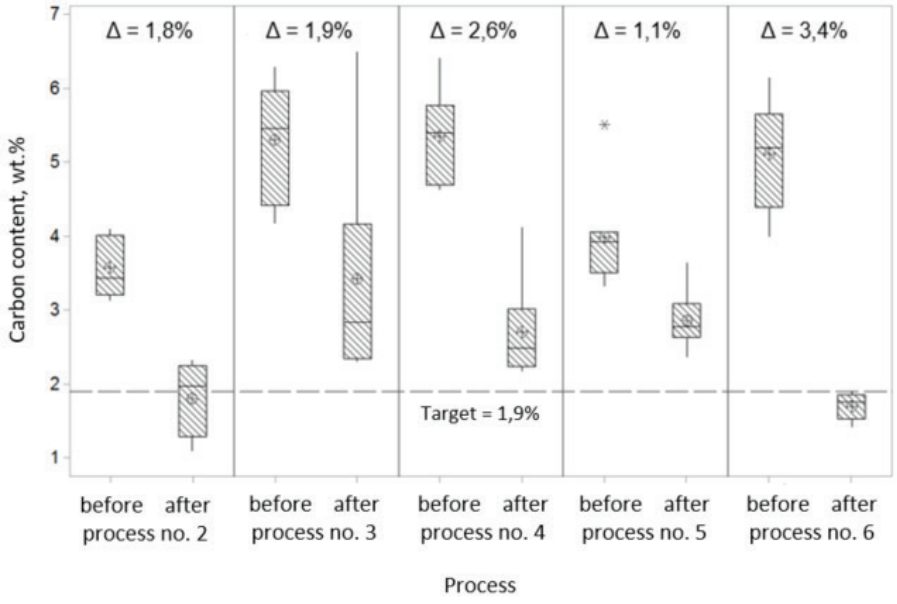

Figure 5. Results of carbon content measurement before and after the decarbonizing process.

sample surface (process no. 5—T = 973 K, Ar 20% + CO_2 80%, τ = 6 h) indicate incorrect conditions for this decarbonizing process.

Hardness measurement was carried out before and after decarbonizing. The results are shown in Figure 11. The values were compared using Student's t-test at a confidence level of 1 – " = 95%. Only for the sample after decarburization process no. 5 (T = 1,123 K, Ar 20% + CO_2 80%, τ = 6 h), a decrease in hardness was observed in a statistically significant way. The change in hardness results from the formation of a corrosion layer with an average depth of 40 mm (Figure 12e).

Studies on the microstructure of ductile iron enabled analysis of the change of phase components of the matrix microstructure, the morphology of graphite precipitates, and the kinetics of corrosion product formation in the surface layer. No change in the morphology of the phase components of the microstructure was found for decarbonizing process no. 2 (T = 1,123 K, Ar 100%, τ = 2 h) (Figure 12b) and process no. 6 (T = 1123 K, Ar 100%, τ = 6 h) (Figure 12f). It was found that decarbonizing under process nos. 3–5, in which the atmosphere of the Ar + CO_2 gas mixture is used, causes the formation of corrosion products in the surface layer (Figure 12c–e). The appearance of the oxide layer on the surface makes the diffusion of elements impossible during the creation of two-layered casting, for which this process was prepared. The thickness of corrosion layer for specimen nos. 3–5 is 4, 9, and 40 mm, respectively.

Table 2. Depth of decarbonized layer and decarbonizing factor

Parameter	No. of process				
	2	3	4	5	6
Depth of decarbonized layer (mm)	100	100	100	180	120
Decarbonizing factor	38.8	29.1	23.8	82.9*	35.9

*The value also consists of the corrosion area.

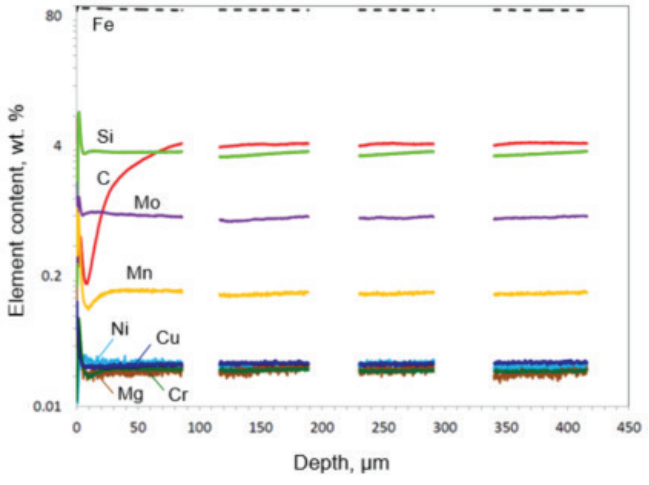

Figure 6. Change of element content in accordance to depth from surface—process no. 2 (T = 1,123 K, Ar 100%, τ = 2 h).

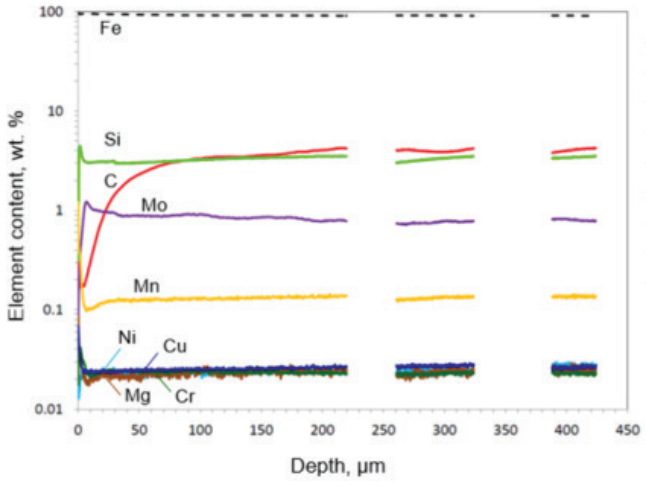

Figure 7. Change of element content in accordance to depth from surface—process no. 3 (T = 1,123 K, Ar 70% + CO_2 30%, τ = 2 h).

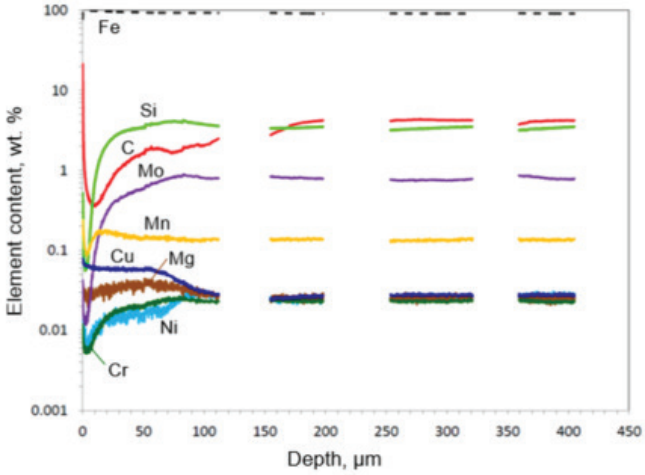

Figure 9. Change of element content in accordance to depth from surface—process no. 5 (T = 1,123 K, Ar 20% + CO_2 80%, τ = 6 h).

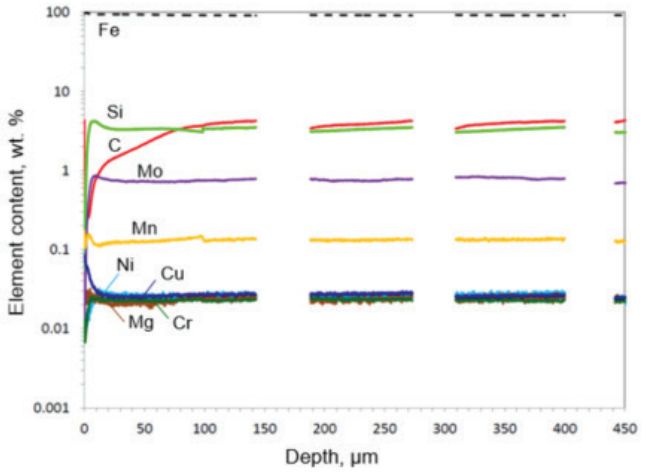

Figure 8. Change of element content in accordance to depth from surface—process no. 4 (T = 1,123 K, Ar 20% + CO_2 80%, τ = 2 h).

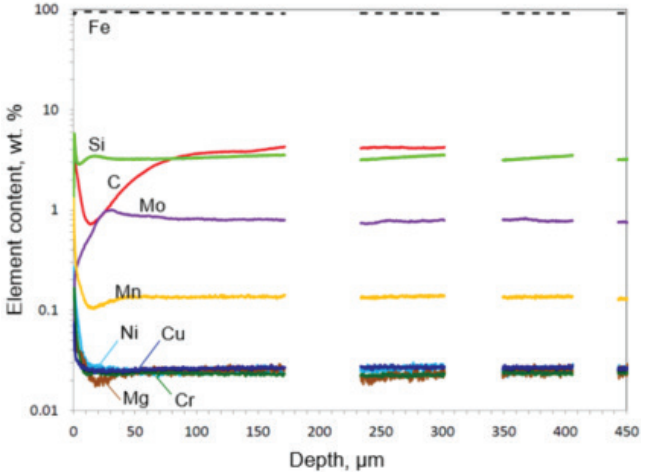

Figure 10. Change of element content in accordance to depth from surface—process no. 6 (T = 1,123 K, Ar 100%, τ = 6 h).

4. Summary and Conclusions

The analysis of the results of the research on the content of elements in the surface layer and also the microscopic studies of its microstructure after the decarbonizing process of ductile iron GJS-XSiMo5-1 allowed to determine that:

the adopted decarbonizing process conditions ensured obtaining a decarbonized layer of GJS-XSiMo5-1 cast iron with a depth of 100 mm (process nos. 2–4) through 120 mm (process no. 6—T = 1,123 K, Ar 100%, τ = 6 h) up to 180 mm (process no. 5—T = 1,123 K, Ar 20% + CO_2 80%, τ = 6 h),

for samples after decarbonizing process nos. 2–4 (corrosion layer 0–9 mm), there was no change in the surface hardness relative to the samples before the hardness process in a statistically significant way, the change in hardness for the sample after process no. 5 is caused by the formation of a corrosion layer of depth 40 mm,

for the adopted assumptions, the acceptance criteria for the decarbonizing process were achieved in process nos. 2 and

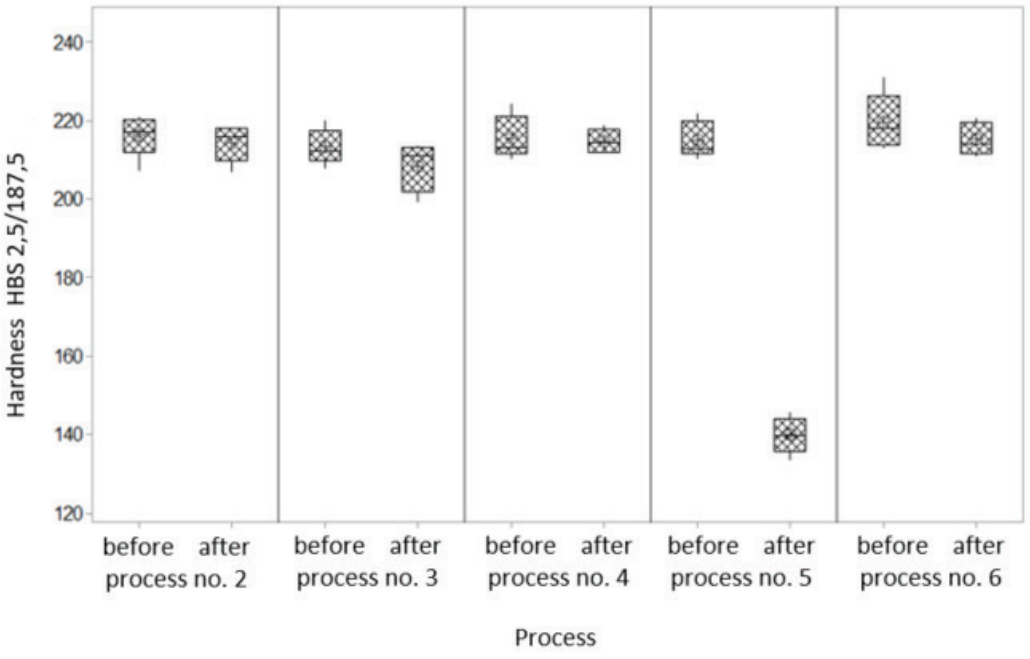

Figure 11. Results of Brinell hardness measurement before and after the decarbonizing process.

6 (content C £ 1.9 wt.%, DC ³ 1.7 wt.%, and no corrosion products),
decarbonizing process in the atmosphere of the Ar + CO_2 gas mixture promotes the activation of the iron corrosion process, the decarbonizing process is in fact a type of oxidation of the surface layer of samples, limited by the use of a protective gas atmosphere, and the appearance of corrosion layer on the surface makes the diffusion of elements during the creation of two-layered casting impossible, for which this process was prepared.
The obtained test results showed that the argon atmosphere ensures that the correct decarbonizing process of GJS-XSiMo5-1 cast iron is 100% argon atmosphere. At the same time, it is believed that increasing the temperature of the decarburization process to 1,373 K (below solidus) increases its predicted effect—the assumed depth of the decarburized layer can be obtained in a shorter time.
The work on this problem is in progress and consecutive results will be published in a succeeding paper.

Acknowledgment

The authors would like to thank Engineer Wojciech Nowak, PhD for performing the glow discharge optical emission spectrometric analyses published in this paper.

References

[1] AVL M.O.V.E iS: A new solutions for the upcoming EU6c – real driving emissions (RDE) legislation. AVL List GmbH, Graz 2014.
[2] United Nations: World Forum for Harmonization of Vehicle Regulations. Proposal for a new global technical regulation on the Worldwide harmonized Light vehicles Test Procedure (WLTP). ECE/TRANS/WP.29/2014/27, 2014.
[3] C.F. WALTON, T.J. OPAR: Iron casting handbook. Iron Casting Society Inc., New York 1981, 57.
[4] J. SZAJNAR, P. WRÓBEL, T. WRÓBEL: Multi-layers castings. *Arch. Found Eng.,* **10**(2010)1, 181-186.
[5] P. HUGGETT, et al.: A novel metallurgical bonding process and microstructural analysis of ferrous alloy composites. *Mater Forum,* **29**(2005), 83-88.
[6] X. GAO, et al.: Effects of temperature and strain rate on microstructure and mechanical properties of high chromium cast iron/low carbon steel bimetal prepared by hot diffusion-compression bonding. *Mater. Des*., **63**(2014), 650-657.
[7] T. KIRMA: Production of coal-crusher hammer heads by bi-metal casting. Master of Science Thesis of Middle East Technical University. Ankara 2008.
[8] S. ZIC, I. DZAMBAS, M. KONIĆ: Possibilities of implementing bimetallic hammer castings in crushing industries. *Metalurgija,* **48**(2009)1, 51-54.
[9] F. BINCZYK, et al.: Krystalizacja żeliwa szarego i stopowego na

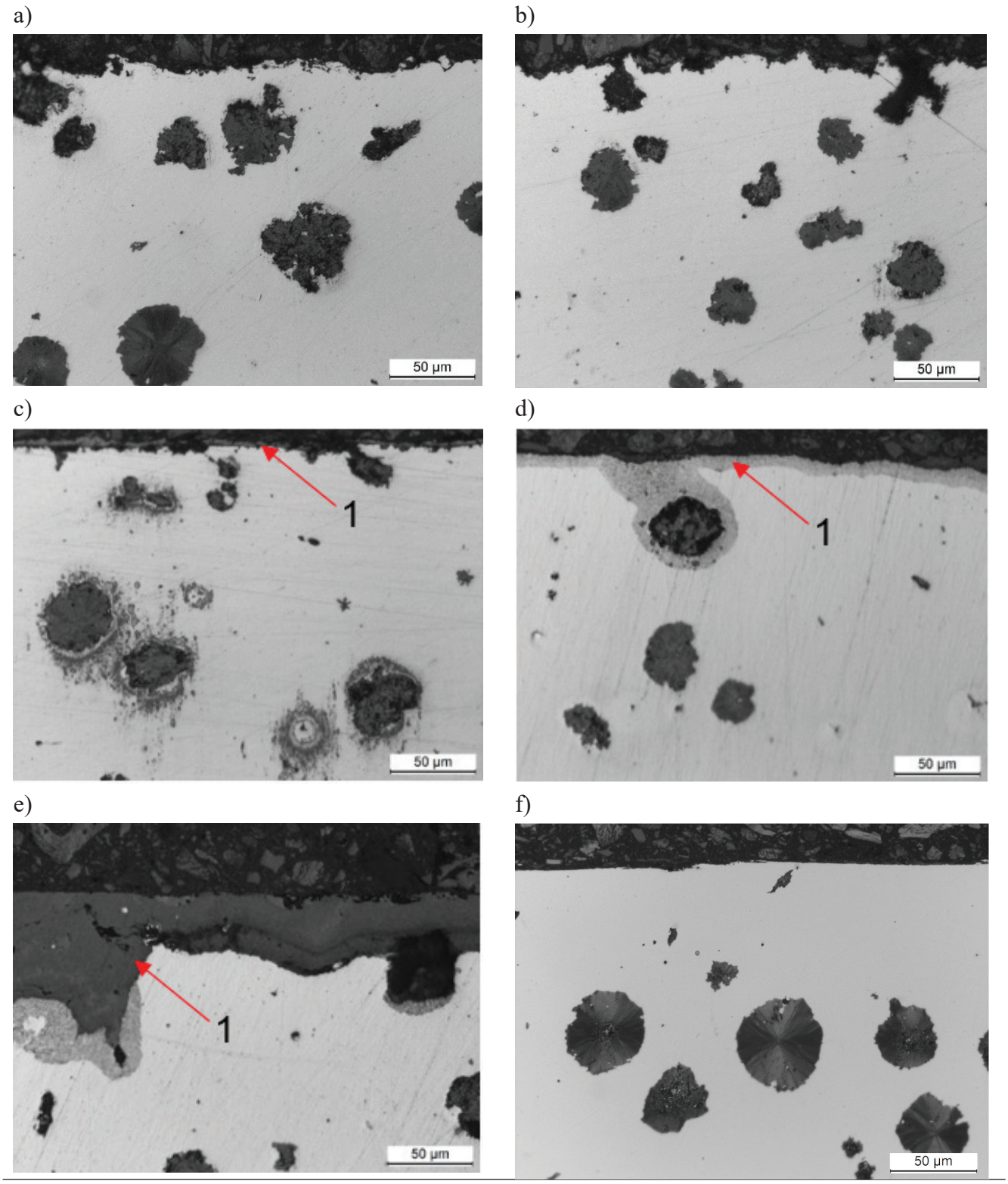

Figure 12. Microstructure of ductile iron GJS-XSiMo5-1: (a) before decarbonizing process, (b) process no. 2 (T = 1,123 K, Ar 100%, τ = 2 h), (c) process no. 3 (T = 1,123 K, Ar 70% + CO_2 30%, τ = 2 h), (d) process no. 4 (T = 1,123 K, Ar 20% + CO_2 80%, τ = 2 h), (e) process no. 5 (T = 1,123 K, Ar 20% + CO_2 80%, τ = 6 h), (f) process no. 6 (T = 1,123 K, Ar 100%, τ = 6 h). Magnification 50´, 1—corrosion layer.

walce dwuwarstwowe. *Archiwum Odlewnictwa,* **1**(2001)1, 34-41.

[10] E. MARUKOVICH, et al.: Study on the possibility of continuous-casting of bimetallic components in condition of direct connection of metals in a liquid state. *Mater. Des.*, **27**(2006), 1016-1026.

[11] F. CALVO, et al.: Diffusion bonding of grey cast iron to Armco iron and a carbon steel. *J. Mater. Sci. Lett.*, **24**(1989), 4152-4159.

[12] T. VIGRAMAN, D. RAVINDRAN, R. NARAYANASAMY: Diffusion bonding of AISI 304L steel to low-carbon steel with AISI 304L steel interlayer. *Mater. Des.*, **34**(2012), 594-602.

[13] P. WRÓBEL, J. SZAJNAR, J. GAWROŃSKI: Kompleksowa ocena warunków powstawania kompozytowej warstwy stopowej na powierzchni odlewu staliwnego. *Archiwum Odlewnictwa,* **4**(2004)14, 593-604.

[14] B. XIONG, C. CAI, B. LU: Effect of volume ratio of liquid to solid on the interfacial microstructure and mechanical properties of high chromium cast iron and medium carbon steel bimetal. *J. Alloys Compd.*, **509**(2011), 6700-6704.

[15] H. SALLAM, et al.: Failure analysis and flexural behavior of high chromium white cast iron and AISI4140 Steel bimetal beams. *Mater. Des.*, **52**(2013), 974-980.

[16] D. BARTOCHA, J. SUCHOŃ, S. JURA: Odlewy warstwowe. *Krzepnięcie Metali i Stopów,* **38**(1998), 151-156.

[17] T. WRÓBEL: Ni and Cr base layers in bimetallic castings. Materials of 20th Anniversary International Conference on Metallurgy and Materials METAL 2011 Brno, Brno 2011, 758-764.

[18] J. SZAJNAR, T. WRÓBEL, A. DULSKA: Manufacturing methods of alloy layers on casting surfaces. *J. Cast. Mater. Eng.*, **1**(2017)1, 2-6.

[19] S. ERTÜRK, et al.: Fabricating of steel/cast iron composite by casting route. *Acta Phys. Pol. A,* **125**(2013)2, 452-453.

[20] I. KISS, S. MAKSAY: Bimetallic cast iron rolls – some approaches to assure the exploitation properties. *Tech. Gaz.,* **17**(2010), 173-178.

[21] A. AVCI, et al.: Mechanical and microstructural properties of low-carbon steel-plate-reinforced gray cast iron. *J. Mater. Process. Technol.*, **209**(2009), 1410-1416.

[22] M. RAMADAN: Interface characterization of bimetallic casting with a 304 stainless steel surface layer and a gray cast iron base. *Adv. Mater. Res.*, **1120-1121**(2015), 993-998.

[23] T. WRÓBEL, M. CHOLEWA: The influence of selected cast parameters on quality of joint in layered castings. *Arch. Foundry Eng.*, **12**(2012)2, 105-110.